Research Article

Training Autoencoder using Three Different Reversed Color Models for Anomaly Detection

Obada Al aama[1], Hakaru Tamukoh[2,*]

[1]Department of Life Science and Systems Engineering, Graduate School of Life Science and Systems Engineering, Kyushu Institute of Technology,
2-4 Hibikino, Wakamatsu-ku, Kitakyushu 808-0196, Japan
[2]Department of Human Intelligence System, Graduate School of Life Science and Systems Engineering, Kyushu Institute of Technology,
2-4 Hibikino, Wakamatsu-ku, Kitakyushu 808-0196, Japan

ARTICLE INFO

ABSTRACT

Autoencoders (AEs) have been applied in several applications such as anomaly detectors and object recognition systems. However, although the recent neural networks have relatively high accuracy but sometimes false detection may occur. This paper introduces AE as an anomaly detector. The proposed AE is trained using both normal and anomalous data based on convolutional neural network with three different color models Hue Saturation Value (HSV), Red Green Blue (RGB), and our own model (TUV). As a result, the trained AE reconstruct the normal images without change, whereas the anomalous image would be reconstructed reversely. The training and testing of the AE in case of RGB, HSV, and TUV color models were demonstrated and Cifar-10 dataset had been used for the evaluation process. It can be noticed that HSV color model has been more effective and achievable as an anomaly detector rather than other color models based on *Z*- and *F*-test analyses.

1. INTRODUCTION

The Artificial Intelligence (AI) is widely used and has been existed over many decades. It uses the information originating from sensors, images, languages and texts. Analyzing this information giving hypothesis leading to make decision [1]. AI can be viewed as a set that contains Machine Learning (ML) and Deep Learning (DL) [2]. DL is often categorized as supervised or unsupervised [3]. Autoencoders (AEs) are one of the DL methods which trained in an unsupervised fashion to automatically extract features of training data [4]. Moreover, anomaly detection is one of the most important applications of AEs [5]. One of the training methods that has been used for anomaly detection is a Convolutional Neural Network (CNN). CNN has been applied in various modern applications, and it is often implemented in image analysis [6], speech and face recognition [7] and autoencoders [8] with great success.

The aim of this study is to use CNN-autoencoder trained with three different color models; Hue Saturation Value (HSV), Red Green Blue (RGB) and our own model (TUV) to improve the detection accuracy especially the anomalous one.

2. RESEARCH CONCEPT

The main concept focuses over using the autoencoder trained with reversed color models in order to detect the anomaly data.

2.1. Autoencoder

Autoencoders are neural networks that aims to copy their inputs to their outputs. It is used to automatically extract features of training data. AEs are applied for object recognition systems that being used the anomaly detectors [5]. To improve a recognition accuracy, the anomaly detectors has the ability to remove anomalous objects before recognition process to reduce misrecognition. AEs are composed of three fully connected layers: input, hidden, and output layers. These layers are trained to reconstruct input data on the output layer as shown in Figure 1.

2.2. Anomaly Detection

The idea in anomaly detection based on machine learning, is to model the normal behavior of data in the training period, and then try to fit the test data using the trained model. In case a large inconsistency is found between the fitted model and the trained model, the test data is regarded as anomalous.

When using autoencoders, which applies dimensionality reduction to the input data, for anomaly detection, we assume that the data contains variables that can be represented in lower dimensions. These variables are also assumed to be correlated with each other and would show significant difference between normal and anomalous samples [9].

There are two types of training data for autoencoder to detect anomaly images; labeled and unlabeled data. Based on the type of

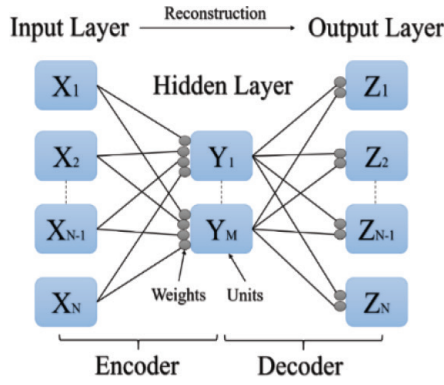*Corresponding author. Email: tamukoh@brain.kyutech.ac.jp*
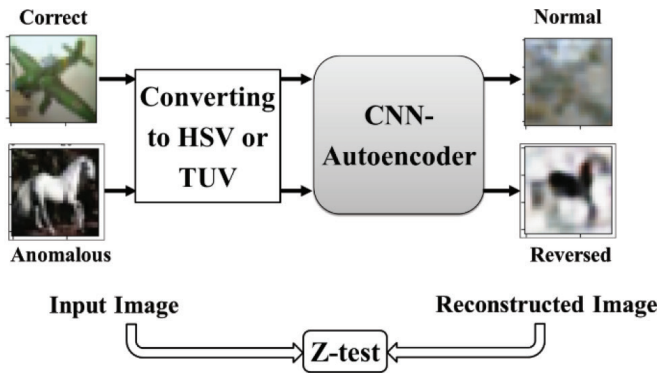
Figure 1 | Structure of autoencoder.

Figure 2 | Block diagram of training method.

Figure 3 | Converting training dataset images, (a) RGB to HSV, (b) HSV to TUV.

Hue calculation (*H*):

$$H = \begin{cases} 0^{\circ} & \Delta = 0 \\ 60^{\circ} \times \left(\dfrac{G' - B'}{\Delta} \bmod 6 \right), & C_{\max} = R' \\ 60^{\circ} \times \left(\dfrac{B' - R'}{\Delta} + 2 \right), & C_{\max} = G' \\ 60^{\circ} \times \left(\dfrac{R' - G'}{\Delta} + 4 \right), & C_{\max} = B' \end{cases} \quad (1)$$

Saturation calculation (*S*):

$$S = \begin{cases} 0, & C_{\max} = 0 \\ \dfrac{\Delta}{C_{\max}}, & C_{\max} \neq 0 \end{cases} \quad (2)$$

Value calculation (*V*):

$$V = C_{\max} \quad (3)$$

where *H*, *S*, and *V* are the component of the HSV image,

$R' = R/255$, $G' = G/255$, $B' = B/255$.

$C_{\max} = \max(R', G', B')$, $C_{\min} = \min(R', G', B')$, and $\Delta = C_{\max} - C_{\min}$

$$T = S \times \sin H \quad (4)$$

$$U = S \times \cos H \quad (5)$$

$$V = V \quad (6)$$

Notice in the case of HSV color model the value range for hue, saturation and value are 0–179, 0–255 and 0–255 respectively.

Secondly, the anomalous data is reversed as a result of the next step as shown in Figure 4, using the following Equations (7)–(9),

$$R_r = 1 - R' \quad (7)$$

$$G_r = 1 - G' \quad (8)$$

$$B_r = 1 - B' \quad (9)$$

Consequently, the AE is trained using the new training dataset based on CNN. The proposed training patterns for AE are as follows: (1) the first case the autoencoder is trained by class 0 as normal and other classes as anomalous, (2) the second case the classes 0 and 1 will be normal and other classes are reversed. Consequently, the number of normal classes will increase for each next case. Finally the autoencoder will be trained with all classes as normal for the last case. Final step of the algorithm is to evaluate the performance

data, the anomaly detection algorithm differs. In case of labeled data, conditional distributions can distinguish between correct and anomalous data. Accordingly, the probability of the conditional distribution determines whether the data is correct or anomalous. On the other hand, a generative model trained with correct data is used as a detector for unlabeled data. The inability of the model to generate a correct output for anomalous data is utilized to detect anomaly.

3. METHODOLOGY

The autoencoder reconstruct the input to the output even if the input was an anomalous data, and the Mean Square Error (MSE) between input and output will be small in case of normal or an anomalous input, and the detection will be difficult especially for the anomalous one. Our goal is to maximize the difference of reconstruction error by reconstructing the anomaly classes reversely. Therefore, the MSE will be bigger and the anomaly detection will be easier as shown in Figure 2.

3.1. Detection Algorithm

The first step of the algorithm is to convert the training dataset images from RGB color model to HSV [10] or TUV as shown in Figure 3a and 3b respectively. Using the Equations (1)–(3) for HSV color model, and Equations (4)–(6) for TUV color model.
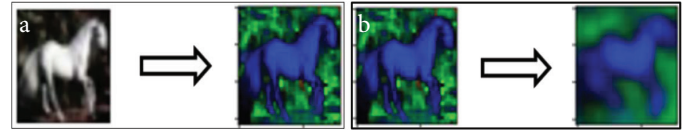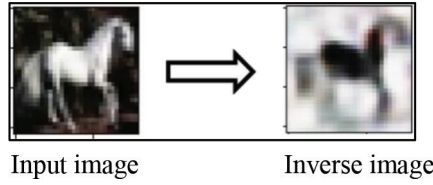
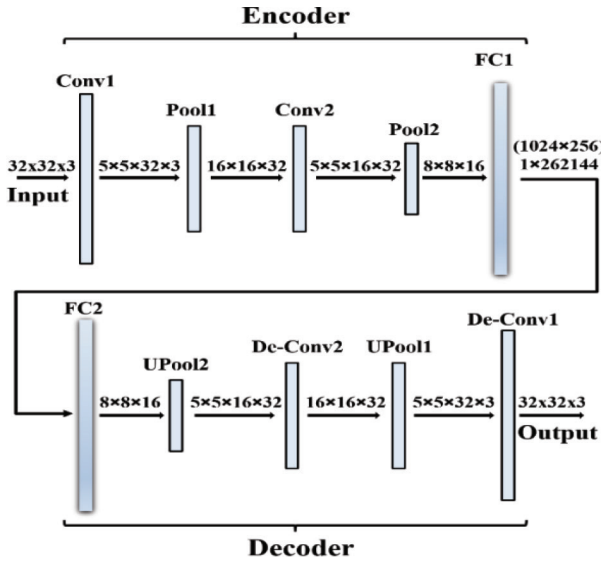**Figure 4** | Inversing the anomalous image.

Figure 5 | Structure of convolutional neural network autoencoder.

of the AE using an inference dataset. Figure 5 illustrates the structure of CNN-autoencoder. As shown in the figure, the input image with size 32 × 32 × 3 is firstly convoluted in the first layer by a 5 × 5 filter.

Consequently, the image dimensions are reduced through a pooling layer from size 5 × 5 × 32 × 3 to size 16 × 16 × 32. Next, another convolution layer is applied followed by a pooling layer to change the size of the image from 5 × 5 × 16 × 32 to 8 × 8 × 16. Finally, the encoding process is finalized with a fully connected layer with the output size of 1 × 262144 (1024 × 256). In order to decode the image, the reverse of the previous process is applied and finally a reconstructed image with the same dimensions as the input image is the same as the output.

3.2. Cifar-10 Dataset

The CIFAR-10 dataset is a set of images that can be used to teach a computer how to recognize objects, it contains RGB images with 32 × 32 pixels' size. It has 10 classes and each class contains a different type of images. The dataset divides into a 50,000 images training set and 10,000 images testing set. Each set has an equal distribution of elements from each one of the 10 classes [11], as shown in Table 1.

Table 1 | The number of images depending on training and testing patterns

Normal labels	The number of images depending on training patterns		The number of images depending on test patterns	
	Normal	**Anomalous**	**Normal**	**Anomalous**
0	5000	45,000	1000	9000
0 and 1	10,000	40,000	2000	8000
0–2	15,000	35,000	3000	7000
0–3	20,000	30,000	4000	6000
0–4	25,000	25,000	5000	5000
0–5	30,000	20,000	6000	4000
0–6	35,000	15,000	7000	3000
0–7	40,000	10,000	8000	2000
0–8	45,000	5000	9000	1000
0–9	50,000	0	10,000	0

3.3. Evaluation of Performance for Autoencoder

For significance validation, both *F*- and *Z*-test were conducted. The *Z*-score value can be calculated based on the following formula (10) [12]:

$$Z = \frac{\bar{x}_1 - \bar{x}_2}{\sqrt{\dfrac{\sigma_1^2}{n_1} + \dfrac{\sigma_2^2}{n_2}}} \quad (10)$$

where $(\bar{x}_1, \bar{x}_2)$ are the average of the input and output pixels values respectively, (σ_1, σ_2) are the standard deviation for the input and output values respectively, (n_1, n_2) are the sample size of the input and output respectively.

A *p*-value is used in hypothesis testing to help accepting or reject the null hypothesis. It is evidence against a null hypothesis. The smaller the *p*-value, the stronger the evidence that you should reject the null hypothesis.

The used hypothesizes are; if *p*-value >0.05, then there is no significant difference between the input and reconstructed image (i.e. considered as Normal).

If *p*-value <0.05, then there is significant difference between the input and reconstructed image (i.e. considered as Anomaly).

4. RESULTS AND DISCUSSION

4.1. Training and Testing Loss

The difference between the test data input images and the reconstructed images were calculated in each epoch. The relationship between the testing loss and the epochs is shown in Figure 6. It is worth mentioning that the value of the test loss is almost similar or close to train loss value and this indicates to a good reconstruction process.
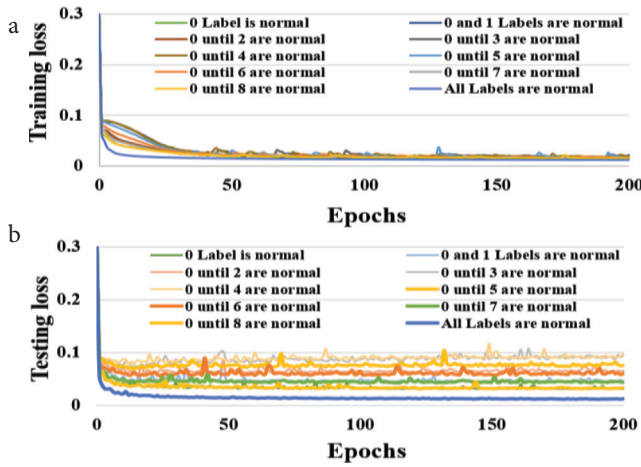
Figure 6 | Training and testing loss against epochs for HSV color model, (a) training loss, (b) testing loss.

Table 2 | *p*-value for class 0 as normal and classes 1–9 as anomalous hypothesis for HSV, RGB and TUV

Classes	Color model type		
	HSV	RGB	TUV
0	0.5819	0.2013	0.2941
1	0.0057	0.0298	0.0012
2	0.0000	0.0100	0.0084
3	0.0076	0.0008	0.0142
4	0.0000	0.0222	0.0010
5	0.0005	0.0182	0.0109
6	0.0053	0.0322	0.0103
7	0.0213	0.0178	0.0478
8	0.0166	0.0424	0.0000
9	0.0267	0.0323	0.0377

4.2. *Z*-test

The *p*-value of each color model was calculated at zero mean value for each class and the results were shown in Tables 2–4 for the three cases; in the first one only class 0 is normal while the rest are anomaly, in the second case classes 0–7 are normal and other classes are anomaly, and in the last one all classes are normal. From Table 2, it is clear that HSV in class 0 is better than RGB and TUV as the *p*-value is 0.5819 which is larger than 0.2013 and 0.2941. This is because in the normal class the difference between input and output image should be small as proven by *p*-value result. In contrast, most of *p*-values of anomaly classes in RGB and TUV are bigger than in HSV which denotes the HSV detects the anomaly classes more effectively than other color models. Similarly, Tables 3 and 4 show that, generally, HSV in all classes is better than RGB and TUV as the detection in HSV is more achievable than other models.

4.3. *F*-test

An anomaly detection performance is usually evaluating by using the *F*-test using the recall and precision as shown in Equation (11) [14]. Accomplishing high recall and high precision

Table 3 | *p*-value for classes 0–7 as normal and classes 8 and 9 as anomalous hypothesis for HSV, RGB and TUV

Classes	Color model type		
	HSV	RGB	TUV
0	0.9473	0.7742	0.1296
1	0.7223	0.1920	0.6506
2	0.9847	0.1795	0.3149
3	0.0760	0.6836	0.1061
4	0.4545	0.1688	0.5228
5	0.5675	0.9366	0.1699
6	0.0882	0.4278	0.8637
7	0.4240	0.2964	0.2785
8	0.0041	0.0000	0.0000
9	0.0012	0.0003	0.0000

Table 4 | *p*-value for classes 0–9 as normal hypothesis for HSV, RGB and TUV color models

Classes	Color model type		
	HSV	RGB	TUV
0	0.4440	0.1899	0.1262
1	0.8405	0.6838	0.1086
2	0.6534	0.7221	0.0653
3	0.7256	0.8480	0.0853
4	0.3155	0.1685	0.0645
5	0.5290	0.1529	0.0792
6	0.8100	0.5489	0.0635
7	0.1732	0.4731	0.4457
8	0.5756	0.3557	0.2570
9	0.8039	0.8849	0.0792

is not easy at the same time because the recall and precision goals are often conflicting.

$$F = 2 \times \left(\frac{\text{Precision} \times \text{Recall}}{\text{Precision} + \text{Recall}} \right) \tag{11}$$

where Precision = True positives/(True positives + False positives), and Recall = True positives/(True positives + False positives).

Figure 7 shows the *F*-test against the threshold for HSV, RGB and TUV respectively. The first mean point in comparing with the previous work is the horizontal range for the *F*-test. This range in the proposed method was small, therefore, the correct threshold for the detection could be defined easily. The second point is that *F*-value in the previous work was bigger in case of RGB than the value in our proposed method and that indicates increasing in the accuracy. In proposed method, the *F*-test for HSV color model is better than other models.

Table 5 represents the comparison between our results and the previous results, the proposed CNN-autoencoder has been trained with three different color models HSV, RGB and TUV, whereas the stacked autoencoder trained with one color model which is RGB. Besides, the reconstruction quality results using the proposed CNN-autoencoder for the same color model (RGB) were better than the reconstruction results using the stacked autoencoder in spite of using the same dataset for the evaluation process.
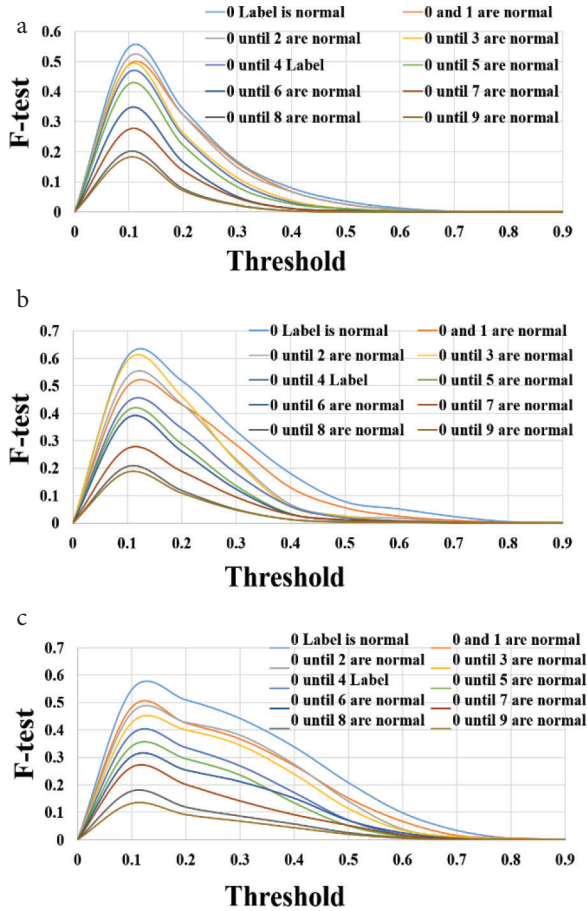
Figure 7 | (a) *F*-test for RGB, (b) *F*-test for HSV, (c) *F*-test for TUV.

Table 5 | General comparison between previous and proposed methods

		Previous method [13]	Proposed method
Training color model		RGB	RGB, HSV and TUV
Structure		Stacked AE	CNN-AE
Dataset		Cifar-10	Cifar-10
Reconstruction quality	• RGB	Moderate	Good
	• HSV	NA	Good
	• TUV	NA	Moderate
F-test	• RGB	Good	Moderate
	• HSV	NA	Good
	• TUV	NA	Moderate
Z-test	• RGB	NA	Moderate
	• HSV	NA	Good
	• TUV	NA	low

5. CONCLUSION

This research investigates the anomaly detection using CNN-autoencoder trained with three different color models. The trained AE has reconstructed the correct input normally, whereas the anomalous input has been reconstructed reversely. The results at 200 epochs training show that HSV color model has been more effective in anomaly detection rather than other models based on *Z*- and *F*-test analyses.

CONFLICTS OF INTEREST

The authors declare they have no conflicts of interest.

REFERENCES

[1] A. Kaplan, M. Haenlein, Siri, Siri, in my hand: Who's the fairest in the land? On the interpretations, illustrations, and implications of artificial intelligence, Business Horizons 62 (2019), 15–25.

[2] O.I. Abiodun, A. Jantan, A.E. Omolara, K.V. Dada, N.A. Mohamed, H. Arshad, State-of-the-art in artificial neural network applications: a survey, Heliyon 4 (2018), e00938.

[3] W. Liu, Z. Wang, X. Liu, N. Zeng, Y. Liu, F.E. Alsaadi, A survey of deep neural network architectures and their applications, Neurocomputing 234 (2017), 11–26.

[4] M. Yousefi-Azar, V. Varadharajan, L. Hamey, U. Tupakula, Autoencoder-based feature learning for cyber security applications, 2017 International Joint Conference on Neural Networks (IJCNN), IEEE, Anchorage, AK, USA, 2017, pp. 3854–3861.

[5] C. Zhou, R.C. Paffenroth, Anomaly detection with robust deep autoencoders, Proceedings of the 23rd ACM SIGKDD International Conference on Knowledge Discovery and Data Mining, ACM, Halifax, NS, Canada, 2017, pp. 665–674.

[6] P. Fonseca, J. Mendoza, J. Wainer, J. Ferrer, J. Pinto, J. Guerrero, et al., Automatic breast density classification using a convolutional neural network architecture search procedure, Proceedings of the Medical Imaging 2015: Computer-Aided Diagnosis, Orlando, FL, USA, 2015, p. 941428.

[7] Y. Sun, X. Wang, X. Tang, Deep learning face representation from predicting 10,000 classes, 2014 IEEE Conference on Computer Vision and Pattern Recognition, IEEE, Columbus, OH, USA, 2014, pp. 1891–1898.

[8] P. Vincent, H. Larochelle, Y. Bengio, P.A. Manzagol, Extracting and composing robust features with denoising autoencoders, Proceedings of the 25th International Conference on Machine learning (ICML), ACM, Helsinki, Finland, 2008, pp. 1096–1103.

[9] V. Chandola, A. Banerjee, V. Kumar, Anomaly detection: a survey, ACM Comput. Surveys 41 (2009), 15.

[10] L. Feng, L. Xiaoyu, C. Yi, An efficient detection method for rare colored capsule based on RGB and HSV color space, 2014 IEEE International Conference on Granular Computing (GrC), IEEE, Noboribetsu, Japan, 2014, pp. 175–178.

[11] A. Torralba, R. Fergus, W.T. Freeman, 80 million tiny images: a large data set for nonparametric object and scene recognition, IEEE Trans. Pattern Anal. Mach. Intell. 30 (2008), 1958–1970.

[12] Website: https://statmagic.info/Content/Help-Content/two-sample-prop.html (accessed July 29, 2019).

[13] A. Suzuki, H. Tamukoh, Reverse reconstruction of anomaly input using autoencoders, 2018 International Symposium on Intelligent Signal Processing and Communication Systems (ISPACS), IEEE, Ishigaki, Okinawa, Japan, 2018, pp. 431–435.

[14] M. Sokolova, N. Japkowicz, S. Szpakowicz, Beyond accuracy, F-score and ROC: a family of discriminant measures for performance evaluation, in: A. Sattar, B. Kang (Eds.), Advances in Artificial Intelligence (AI), Springer, Berlin, Heidelberg, 2006, pp. 1015–1021.

AUTHORS INTRODUCTION

Mr. Obada Al aama

He graduated from Al-Baath University Department of Communication and Electronics Engineering, Syria, in 2013. He received Master of Engineering degree from Kyushu Institute of Technology, Japan, in 2019. His research interests include image processing, deep learning and neural networks.

Associate Prof. Hakaru Tamukoh

He received the B.Eng. degree from Miyazaki University, Japan, in 2001. He received the M.Eng. and the PhD degree from Kyushu Institute of Technology, Japan, in 2003 and 2006, respectively. He was a postdoctoral research fellow of 21st century center of excellence program at Kyushu Institute of Technology, from April 2006 to September 2007. He was an Assistant Professor of Tokyo University of Agriculture and Technology, from October 2007 to January 2013. He is currently an Associate Professor in the Graduate School of Life Science and System Engineering, Kyushu Institute of Technology, Japan. His research interest includes hardware/software complex system, digital hardware design, neural networks, soft-computing and home service robots. He is a member of IEICE, SOFT, JNNS, IEEE, JSAI and RSJ.